PAPER-BASED ACOUSTIC TRANSDUCERS WITH TUNABLE RESONANCE

BY

SANDESH GOPINATH

A thesis submitted to the

Graduate School-New Brunswick

Rutgers, The State University of New Jersey

in partial fulfillment of the requirements

for the degree of

Master of Science

Graduate Program in Mechanical and Aerospace Engineering

written under the direction of

Professor Aaron D. Mazzeo

And approved by

_____

_____

_____

New Brunswick, New Jersey

October 2015

ABSTRACT OF THE THESIS

Paper-based Acoustic Transducers with Tunable Resonance

By Sandesh Gopinath

Thesis Director:

Aaron D. Mazzeo

This thesis describes the use of metallized paper as an electrostatically-driven, tunable acoustic source. Cutting the paper into different patterns and shapes alters the frequency response of the vibrating membranes. This work includes the experimental characterization of five patterns with distinct responses and provides qualitative simulations to verify the observed behaviors. With this unique platform, the author demonstrates a potential application – similar to barcode scanning – that identifies objects based on their acoustic signatures. In addition, it is possible to detect changes in acoustic signatures as a result of placing slits in the membranes, which suggests the platform may be applicable to anti-tampering or security-based technologies. Changes in the measured acoustic amplitudes of vibration were as large as 50%, and for cases of intentionally patterned devices, detection of tampering and incisions in membranes resulted in changes in mechanical resonance of 12%. Overall, this platform suggests the potential viability for a new class of smart packaging that makes use of metallized paper as an environmentally benign and low-cost material.

Acknowledgements

I would like to thank my advisor Aaron D. Mazzeo for giving me the opportunity to work on this project. He has encouraged me to push my limits and I thank him for all his patience and belief in my abilities.

A sincere thanks and appreciation to my fellow lab mates Jingjin Xie and Yanjun Wang for helping me complete my research. I would like to express my gratitude and appreciation to Prof. Haim Baruh for his suggestions. I would like to thank Prof. Haym Benaroya and Prof. Assimina A. Pelegri for taking time out to be part of the thesis review committee.

Most importantly, I would like to thank my family and friends who have been with me through all the ups and downs and encouraged me to keep on moving forward.

Sandesh Gopinath

Rutgers University

October 2015

Dedication*:*

Dedicated to my Family,

Sarasa Gopinath, Madathil Gopinath and Girish Gopinath

Without whose support my work would not have been possible.

Table of Contents

Abstract ii

Acknowledgements iii

Dedication iv

Chapter 1. Introduction 1

1.1. Idea and Motivation 1

1.2. Metallized Paper as a Material for Electrostatics and Acoustics 2

1.3. Introduction to speakers 2

1.4. Electrostatic Theory 3

1.5. Overview of the Thesis 4

Chapter 2. Experimental Design 6

2.1. Electrostatic Excitation of Membranes 6

2.2. Experimental setup 7

2.3. Signal Processing and Characterization of Acoustic Signatures 11

Chapter 3. Acoustic Response of Patterned Metallized paper 15

3.1. Introduction 15

3.2. Discussion 15

Chapter 4. Applications 19

4.1. Loudspeaker 20

4.1.1. Experimental Setup 20

4.1.2. Results and Discussions 21

4.2. Barcode Scanner 27

4.2.1. Introduction 27

4.2.2. Experimental setup 27

4.2.3. Results and discussions 29

4.3. Security and anti-tamper device 34

4.3.1. Motivation 34

4.3.2. Experimental Setup 34

4.3.3. Results and Discussions 36

Chapter 5. Conclusions and Future Work 39

5.1. Conclusions 39

5.2. Future Work 39

References 41

List of Figures

Figure 1: (a) Plots of applied input voltage and electrostatic force versus time on a conductive membrane parallel to a grounded electrode. The forcing frequency is twice the input frequency. (b) Positions of the membranes at different moments in a single cycle of electrostatically forced oscillation. 7

Figure 2: Schematic for the experimental setup and hardware. The computer system controls the NI-cDAQ, which sends a signal to the amplifier and logs the applied voltage and resulting audio. The electrodes are perpendicular to the axis of the microphone and are 5 inches (12.7 cm) away from the microphone. Both the paper-based device and microphone are at the center of the box to have acoustic symmetry. 8

Figure 3: (a) Schematic showing the layers of metallized paper. (b) Configuration of electrodes with the fixed grounded electrode and active electrode free to vibrate. (c) SolidWorks assembly showing the stacked view of the components. (d) Photo of the experimental setup described in B and C. 9

Figure 4: (a) Voltage sent to the amplifier from the NI 9263 with 16 distinct applied frequencies (0.5 kHz to 8 kHz) with 0.5-sec pauses between applied inputs. (b) Output voltage monitored from the amplifier with decreasing output at higher frequencies. The actual potential applied to the device was 1000X that shown. (c) Difference in the monitored amplitudes between the applied and delivered potential across the high-voltage amplifier. 12

Figure 5: (a) Acoustic response of a paper-based membrane for an input electrical signal of 2 kHz. (b) Magnified view of the audio sample in (a) showing individual signals with data points. (c) FFT of audio sample in (a) showing accurate measurement of the amplitude of the acoustic pressure response. 13

Figure 6: (a), (b), (c), (d) and (e) are images of patterned metallized paper used for experiments. Metallized paper was A-238 (thickness of 110 um) from AR Metallizing. (f), (g) and (h) show the acrylic fixtures used to clamp the metallized paper membranes along their edges. Clamp (f) was

used for membrane (d); clamp (g) was used for membranes (a), (b), and (c); and clamp (h) was used for membrane (e). 15

Figure 7: (a), (b), (c), (d) and (e) are frequency response plots for the respective geometric patterns shown in Figure 3 (a), (b), (c), (d) and (e). The error bars are ± 1 standard deviation with seven distinct samples taken on the same device for each pattern. 17

Figure 8. FFT showing frequency responses for patterns 1 and 2 in Figure 3 (a) and (b), respectively using paper with a thickness of 155 um. 21

Figure 9: Audio outputs from devices playing "Mary Had a Little Lamb". (a) Musical staff for "Mary Had A Little Lamb" with notes that are octaves below those delivered to the devices. (b) Acoustic response of Pattern 1 to electrical signals in the frequency range of 1 kHz-2 kHz (i.e., A=1.76 kHz) with acoustic responses in the frequency range of 2 kHz-4 kHz. (c) Acoustic response of Pattern 1 to electrical signals in the frequency range of 4 kHz-8 kHz (i.e., A=3.52 kHz) with acoustic responses in the frequency range of 8 kHz-16 kHz. (d) Acoustic response of Pattern 2 to electrical signals in the frequency range of 1 kHz-2 kHz (i.e., A=1.76 kHz) with acoustic responses in the frequency range of 2 kHz-4 kHz. (e) Acoustic response of Pattern 2 to electrical signals in the frequency range of 4 kHz-8 kHz (i.e., A=3.52 kHz) with acoustic responses in the frequency range of 8 kHz-16 kHz. 22

Figure 10: Audio outputs from devices playing "Twinkle Twinkle Little Star". (a) Musical staff for "Twinkle Twinkle Little Star" with notes that are octaves below those delivered to the devices. (b) Acoustic response of Pattern 1 to electrical signals in the frequency range of 1 kHz-2 kHz (i.e., A=1.76 kHz) with acoustic responses in the frequency range of 2 kHz-4 kHz. (c) Acoustic response of Pattern 1 to electrical signals in the frequency range of 4 kHz-8 kHz (i.e., A=3.52 kHz) with acoustic responses in the frequency range of 8 kHz-16 kHz. (d) Acoustic response of Pattern 2 to electrical signals in the frequency range of 1 kHz-2 kHz (i.e., A=1.76 kHz) with acoustic responses in the frequency range of 2 kHz-4 kHz. (e) Acoustic response of Pattern 2 to electrical signals in the frequency range of 4 kHz-8 kHz (i.e., A=3.52 kHz) with acoustic responses in the frequency range of 8 kHz-16 kHz. 23

Figure 11: Audio output from Patterns 1 and 2, playing a variation of “Twinkle Twinkle Little Star” which has alternating notes in high and low frequencies. (a) Musical staff for “Twinkle Twinkle Little Star variation”, which has notes in the treble clef and bass notes played alternately. (b) Measured acoustic response for Pattern 1 with the notes in the treble clef ranging from 4 kHz-8 kHz and bass notes ranging from 1 kHz- 1.76 kHz. (c) Measured acoustic response for Pattern 2 with the notes in the treble clef ranging from 4 kHz-8 kHz and bass notes ranging from 1 kHz-1.76 kHz. 24

Figure 12: (a) Metallized paper from AR Metallizing A-238 (thickness of 110 um) with four 20-mm x 20-mm patterns cut using a laser cutter to the main component of the scanner. (a) Photo of experimental setup. (b) Scanner consisting of patterned metallized paper as an active electrode and a microphone perpendicular to plane of membrane. (c) Acrylic base with four Barcodes consisting of four grounded pieces of metallized paper (same as (a)) with electrical connections made using thin-grade copper wires and conductive adhesive. 27

Figure 13: Schematic showing working of demonstration where each barcode excites only one of the patterns on the scanner membrane in Figure 13 (a). 29

Figure 14: Snapshots of demonstration showing detection of barcodes and the position of scanner. (a), (b), (c), and (d) show detection of barcodes 1, 2, 3 and 4 respectively as shown on the screen by using a LabVIEW program. 30

Figure 15: (a) Plot displaying responses of four barcode/patterns made from 110 um-thick metallized paper with the patterns easily distinguishable at 5 kHz. (b) The error bars show the upper and lower limits (thresholds) of acoustic pressure set in LabVIEW for detection of the four barcodes at 5 kHz. 31

Figure 16: Images of 110-um thick metallized paper from AR Metallizing with slots/cuts, along with measured frequency responses. (a) Image of a sheet of metallized paper without a cut. (b) Image of a sheet with a 1-mm x 10-mm slot. (c) Image of a sheet with a 1-mm x 20-mm slot. (d) Image of a sheet with a 1-mm x 30-mm slot (e) Plot comparing frequency responses of patterns in (a), (b), (c) and (d). 34

Figure 17: Setup description for demonstration/anti-tamper video using metallized paper with a thickness of 110 um. (a) Image of experimental setup with scalpel, electrode setup and microphone. (b) Schematic describing the process of incision made using a scalpel on metallized paper. (c) Image of paper without a cut. (d) Image of paper with cut. 36

Figure 18: Snapshots of the demonstration for an input voltage of ± 2 kV at 4 kHz. (a) Image showing the amplitude of acoustic pressure at 0.0865 Pascals with no incision. (b) Image showing process of cutting the paper with a scalpel. (c) Image showing the amplitude of acoustic pressure at 0.0990 Pascals with incision. 37

Chapter 1.

Introduction

Recent advances in paper-based electronics have evolved from patterning fluidic channels in microfluidics [1] to patterning conductive traces for electrical applications [2]. Applications of paper-based electronics include oscillators with organic electronics [3], transistors [4]–[6], capacitive touch pads [7], supercapacitors [8], thermochromic displays [9], electrochromic displays [10], solar cells [11], and speakers [12].

1.1. Idea and Motivation

While work by He Tian, et al. [12] demonstrated the potential of using graphene on a paper-based substrate to produce sound using the thermoacoustic effect in the ultrasonic range, there is generally a lack of research on the coupling between the acoustic resonance of paper-based substrates and their design. The present work uses the principles and basics of electrostatic attraction with alternating potential to induce vibration on paper-based membranes. This vibration – ranging from 1 kHz to 16 kHz – results in production of audible acoustic waves. To tune the resonance of the devices, we cut the paper-based membranes with varied patterns and measure the changes in the acoustic response under electrostatic forcing. The operation of these devices is similar to that of a single-sided electrostatic transducer that might employ a flexible, metallized membrane.

1.2. Metallized Paper as a Material for Electrostatics and Acoustics

Metallized paper is a ubiquitous and environmentally benign commodity. It is also, durable, and disposable [7]. Being thin and lightweight in construction, we can configure its structure using a laser cutter. Metallized paper (A-238 from AR Metallizing-A Nissha Company) serves as the material for both the vibrating membrane and the grounded electrode in the devices studied in this thesis. The sheets of paper consist of three functional layers: a base cellulose layer that serves as a physical support, a middle layer of evaporated aluminum, and a thin top layer of a protective polymer coating. The conductive layer is ~ 10 nm thick and the paper has a combined thickness of 110 um. The metallized paper used in the experiments support oscillating high voltages of ± 2 kV (500 Hz to 8 kHz) without significant deterioration. Metallized paper is inexpensive and the samples used in the experiments cost less than US$0.50 per square meter when bought in bulk and is in commercial use as a material for packaging and gift wrapping.

1.3. Introduction to speakers

A speaker is a device that converts electrical signals into audible sound waves. The types of speakers available include horns, electrodynamic speakers, flat-panel speakers, plasma-arc speakers, and piezoelectric speakers [13]. Electrodynamic speakers are the most commonly available and use an electromagnetic coil connected to a diaphragm. Alternating electrical current running through the electromagnetic coil in the

presence of a permanent magnetic field drives the diaphragm back and forth. The back-and-forth action of the diaphragm then creates alternating acoustic pressure or sound waves. In contrast to speakers driven with electromagnetic voice coils, an electrostatic speaker employs high electric fields to drive a diaphragm back and forth. These flat-panel speakers have their diaphragm, or thin membrane, stretched between two rigid electrodes. The membrane typically has polarity or a constant electret-based charge. Alternating the polarity of high voltage produces an electric field to push the charged membrane back and forth (see next section for more detail).

Speakers come in different sizes because it is nearly impossible to make one piston-like driver that can reproduce sound waves over the entire frequency range of human hearing (20 Hz to 20 kHz). Tweeters are the small drivers that produce the highest frequencies with the shortest wavelengths, while woofers are the largest drivers since they produce the lowest frequencies with the longest wavelengths. Certain mid-range drivers are also available, which have a frequency response in between tweeters and woofers.

1.4. Electrostatic Theory

An electrostatic speaker or transducer has three components: a stator, a diaphragm, and a spacer. It is assembled with a diaphragm sandwiched between two stators. The stators are usually perforated metal sheets coated with an insulator. Stretched between the two stators is the diaphragm, which is usually a very thin plastic film with an electrically conductive material impregnated in it. The stators are alternately

positively and negative charged (i.e., when one is positive the other is negative), while a high voltage power supply applies a constant positive or negative charge on the diaphragm. Alternatively, electrostatic transducers have a permanently polarized diaphragm (electret) which does not require an external voltage supply [14]. As like charges repel and opposite charges attract each other, a negative stator pulls a positively charged diaphragm towards itself and the positive stator repels it. This motion of the diaphragm creates a sound and converts the electrical input signal to acoustic output. Compared to a conventional cone speaker, an electrostatic speaker has low levels of distortion and a smooth pressure response that is free from peaks and valleys in the curve displaying relative response as a function of frequency [15]. This smooth/flat response is primarily because the moving mass in a conventional electrodynamic speaker is tens or hundreds of grams, while the diaphragm in an electrostatic speaker weighs only a few milligrams.

1.5. Overview of the Thesis

This thesis consists of five chapters, with the first being this introductory chapter. Chapter 2 explains the experimental setup, the configuration of electrodes, and the associated physics. Chapter 3 discusses the different patterns created on the metallized paper, their acoustic response with focus on. Chapter 4 deals with the application of the novel technique discussed in Chapter 3 to the creation of inexpensive acoustic speakers with tunable responses dependent on patterned geometries. Chapter 4 also describes an acoustic processing system similar to a barcode-scanner, which might have future use in

security or anti-tamper devices. Finally, Chapter 5 shares conclusions derived from the research and presents potential future directions.

Chapter 2

Experimental Design

Electrostatic transducers can be either "single-sided" – electrostatic forces pull the diaphragm in only one direction – or "push-pull" – electrostatic forces push and pull the diaphragm to both sides of its position of static equilibrium [15]. The present design is a single-sided electrostatic transducer with a fixed electrode, or stator, and an active vibrating electrode. The device is in a parallel-plate configuration with both electrodes made of metallized paper. The configuration of electrodes is similar to designs employed by Arthur Janszen in his early designs of electrostatic speakers [16].

2.1. Electrostatic Excitation of Membranes

The application of high AC voltage between a paper-based electrode and a fixed grounded electrode in a parallel-plate configuration causes the paper-based membrane to vibrate and produce sound. These charged parallel electrodes separated by a small distance form a parallel-plate capacitor. The magnitude of the electrostatic force applied on the diaphragm is given by

$$F = \frac{1}{2}\varepsilon_0 A \frac{V^2}{d^2}, \tag{1}$$

where ε_0 is the electrical permittivity of free space, A is the area of the electrode, V is the voltage applied between the electrodes, and d is the distance between the electrodes. The

force between the plates is attractive and the frequency at which the membrane vibrates is twice that of the input signal frequency (Figure 1).

2.2. Experimental setup

We enclosed the electrodes and the microphone in a damped acoustic chamber, which was a closed wooden box – 1.25 feet x 1.5 feet x 1.25 feet (0.38 m x 0.46 m x 0.38 m) – lined with 1-inch thick foam for soundproofing (Figure 2). The lid of the box had small grooves to facilitate wired connections to the electrodes and the microphone, and we placed the microphone with its axis perpendicular to the face of the electrode. The microphone was 5 inches (12.7 cm) away from the electrode setup to prevent damage from the electric field created near the active electrode. The electrode setup consisted of a bottom electrode and a top electrode both made of metallized paper. The paper consist of three functional layers: a base cellulose layer that serves as a physical support, a middle layer of evaporated aluminum, and a thin top layer of a protective polymer coating (Figure 3 (a)). A conductive silver adhesive smeared on a small region on the top layer of the paper provided an electrical connection between the paper and the circuit. A metal screw, with its head in contact with a smeared area of conductive adhesive, provided an electrical connection via alligator clamps. The bottom metallized paper constituted the grounded electrode and the top piece was the active electrode, which drew the electrical current and underwent vibration. We used double-sided tape to fix the bottom electrode

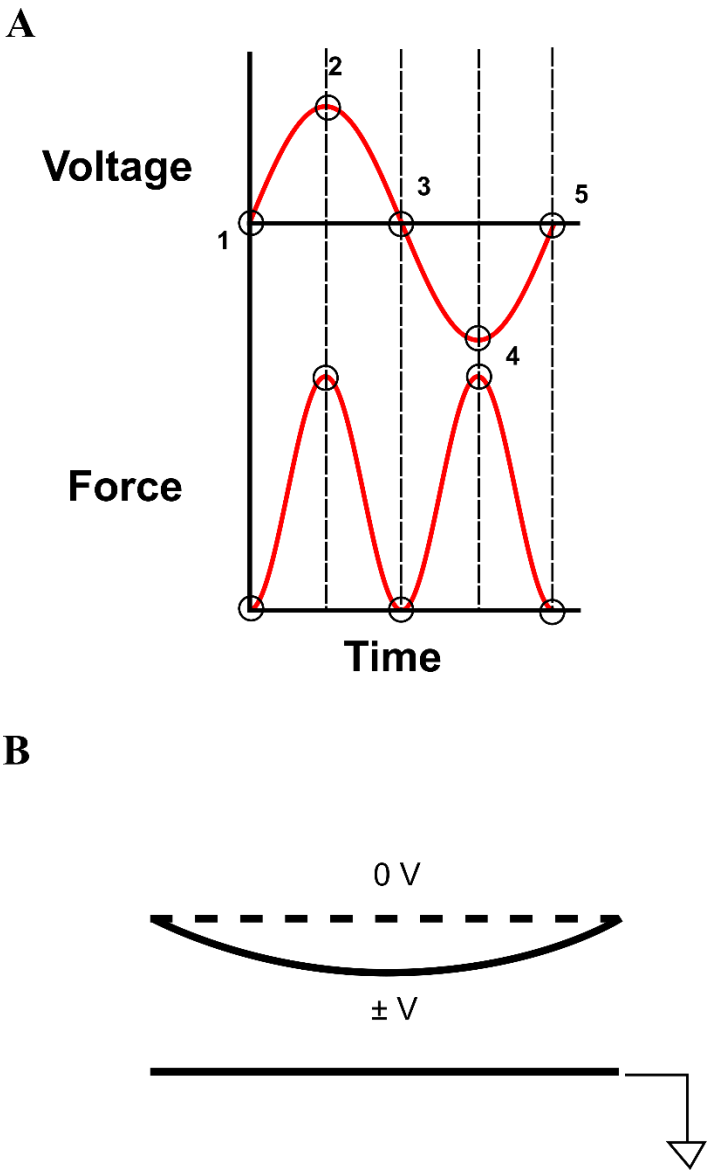

Figure 1: (a) Plots of applied input voltage and electrostatic force versus time on a conductive membrane parallel to a grounded electrode. The forcing frequency is twice the input frequency. (b) Positions of the membranes at different moments in a single cycle of electrostatically forced oscillation.

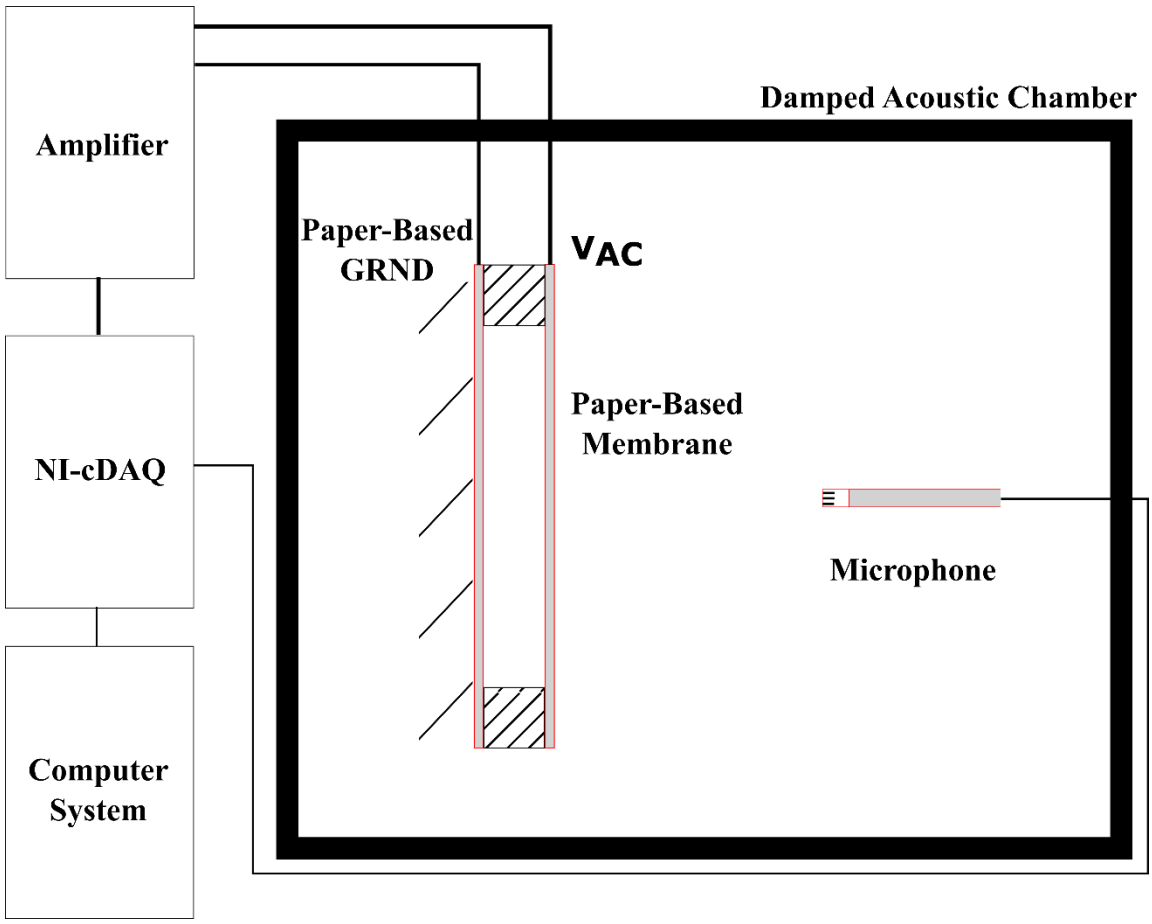

Figure 2: Schematic for the experimental setup and hardware. The computer system controls the NI-cDAQ, which sends a signal to the amplifier and logs the applied voltage and resulting audio. The electrodes are perpendicular to the axis of the microphone and are 5 inches (12.7 cm) away from the microphone. Both the paper-based device and microphone are at the center of the box to have acoustic symmetry.

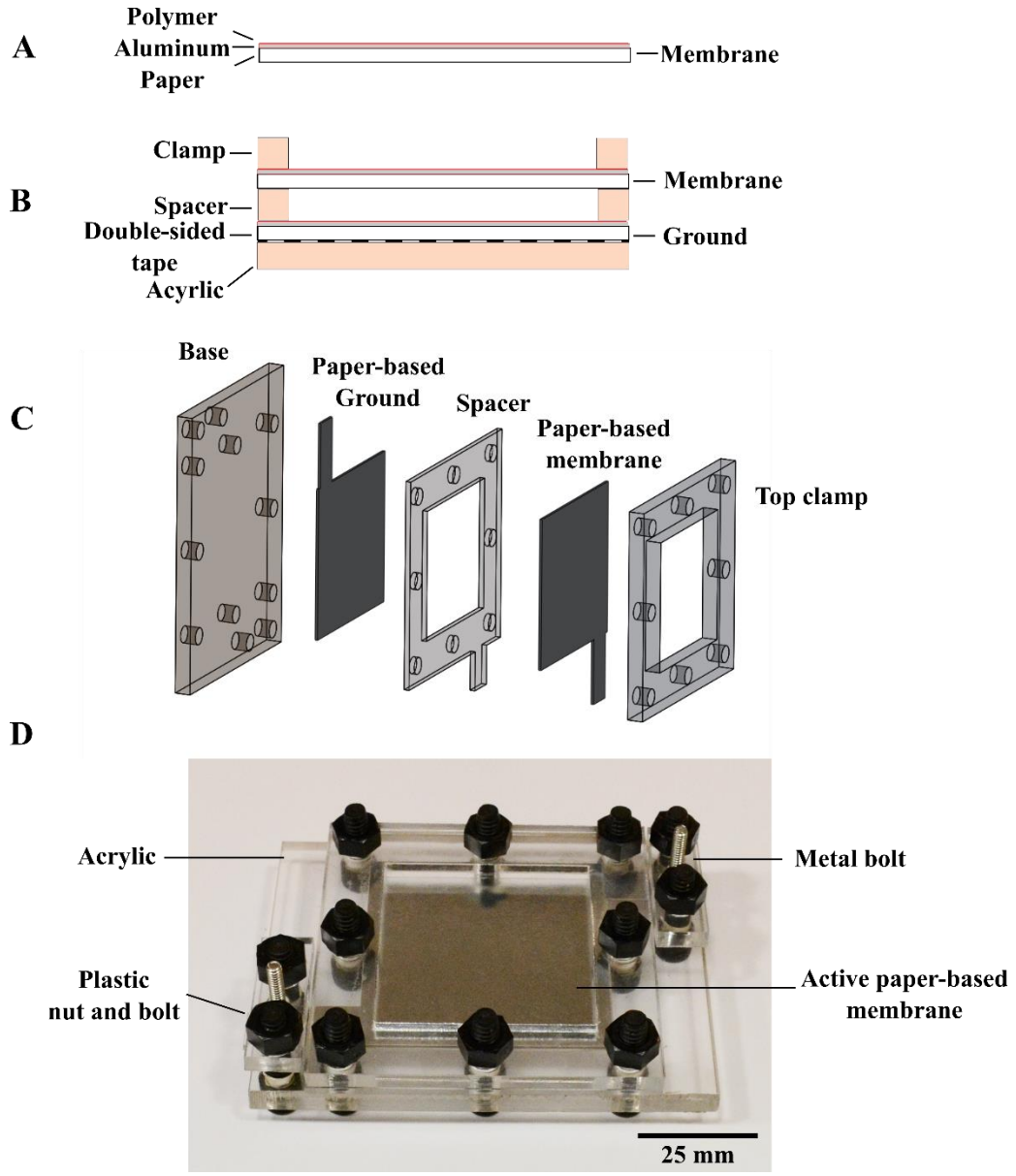

Figure 3: (a) Schematic showing the layers of metallized paper. (b) Configuration of electrodes with the fixed grounded electrode and active electrode free to vibrate. (c) SolidWorks assembly showing the stacked view of the components. (d) Photo of the experimental setup described in B and C.

to the base acrylic piece and clamped the top electrode along its perimeter/edges (Figure 3 (a)). We used nylon socket-head screws and nuts (Figure 3 (d)) to clamp the membrane and secure the electrodes. While we did not monitor the tension in the membrane and the clamping force, we used the same clamping procedure in the experiments. The housing for the electrodes consisted of 6-mm thick sheets of acrylic and a 2-mm thick acrylic spacer to separate the electrodes. We prevented the dielectric breakdown of air by using electric fields less than the dielectric strength of 6 MV/m for air across this 2-mm gap. The material properties of the membranes are unknown. Properties like Young's modulus [17], Poisson's ratio [18], and density [19] can be calculated in the future from material testing and will be important in performing simulations.

2.3. Signal Processing and Characterization of Acoustic Signatures

We used hardware and software (LabVIEW) from National Instruments for data acquisition. A NI 9263 module supplied electrical signals to the high voltage amplifier, and a NI 9215 module monitored the voltage output from the amplifier. We employed a Trek *10/10* amplifier, which amplified the input signal using a gain of 1000V/V. A Brüel & Kjær type 4961 microphone with a sensitivity of 60 mV/Pa and a sampling rate of 51.2 kHz/s converted measured acoustic pressures to electrical signals. A NI 9234 module recorded these electrical signals from the microphone for later analysis. We sampled the acoustic signals at a rate of 100 kHz. All the modules were connected and controlled via a NI cDAQ 9184, which had a chassis to house the modules and connect to a desktop computer via Ethernet.

The LabVIEW program performed a frequency sweep by generating a single frequency signal that was one second long, followed by a 500-millisecond pause before moving to the next frequency. The program simultaneously recorded the output from the amplifier and the microphone. The voltage generated in LabVIEW was at 16 individual frequencies from 500 Hz to 8 kHz in increments of 500 Hz with pauses between frequencies. The amplitude of the signal to the amplifier was ± 2 Volts. Due to a bandwidth up to 5 kHz, the amplifier attenuated output signals for frequencies higher than 5 kHz. To compensate for this attenuation in voltage, we made calibrated measurements and scaled voltages appropriately based on data collected in Figure 4.

By performing a Fast Fourier Transform (FFT) on the output audio signal in MATLAB, we detected the frequency components of the measured signals. As the recorded audio contained experimental measurements at 16 distinct frequencies, we broke the recording into 16 individual portions of time and performed FFTs on them separately. The FFT used 0.8-second segments from the 1-second clips at the 16 distinct frequencies. It was important that the FFT not include the pauses between each clip which might have attenuated the magnitude of acoustic pressure. Figure 5 demonstrates the efficacy of performing an FFT to characterize the amplitude of a measured audio wave.

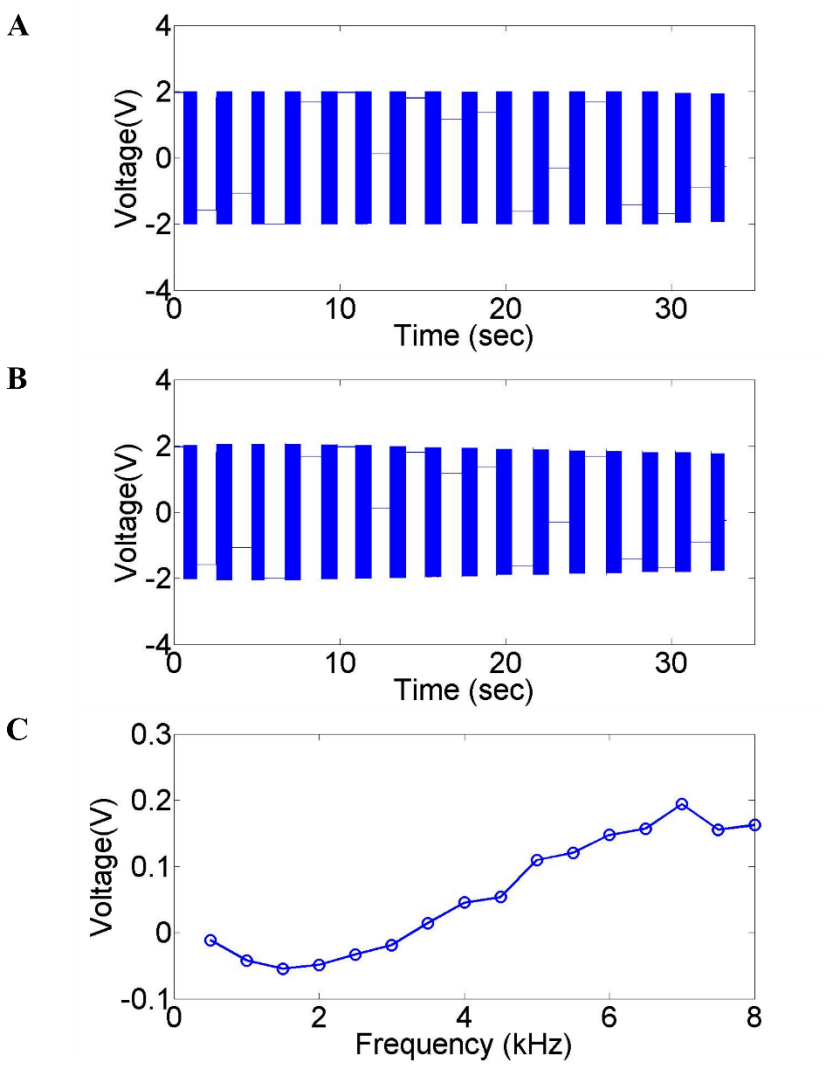

Figure 4: (a) Voltage sent to the amplifier from the NI 9263 with 16 distinct applied frequencies (0.5 kHz to 8 kHz) with 0.5-sec pauses between applied inputs. (b) Output voltage monitored from the amplifier with decreasing output at higher frequencies. The actual potential applied to the device was 1000X that shown. (c) Difference in the monitored amplitudes between the applied and delivered potential across the high-voltage amplifier.

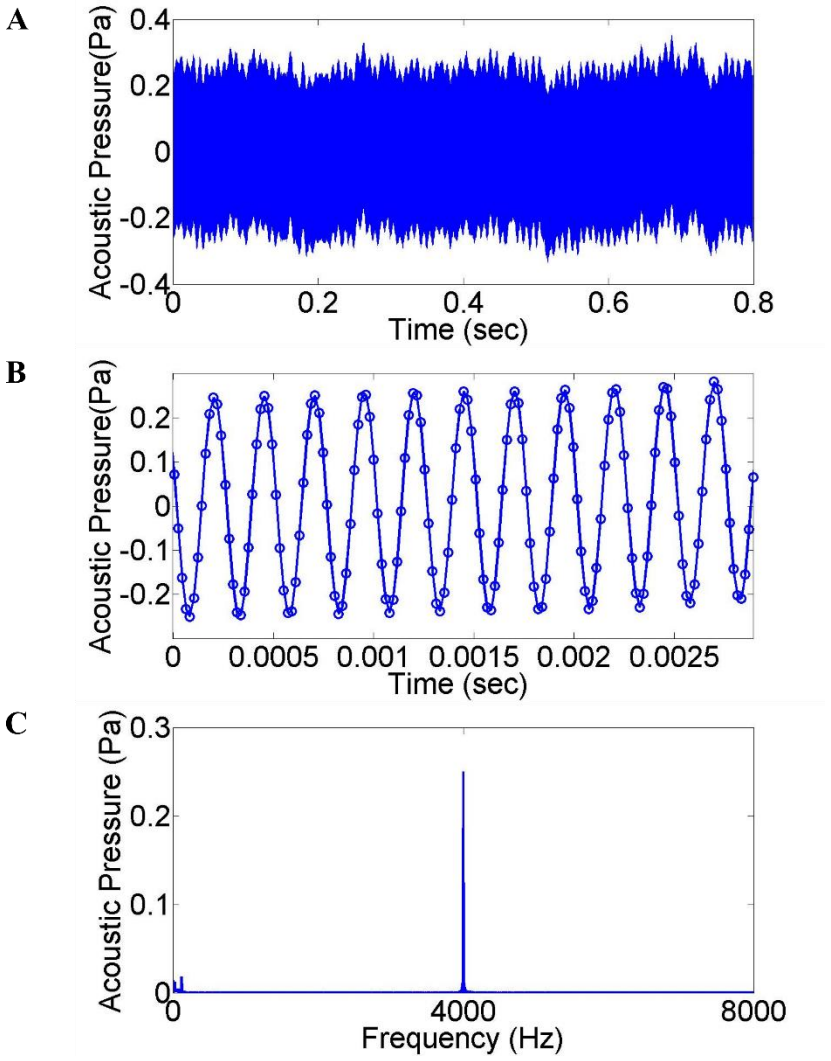

Figure 5: (a) Acoustic response of a paper-based membrane for an input electrical signal of 2 kHz. (b) Magnified view of the audio sample in (a) showing individual signals with data points. (c) FFT of audio sample in (a) showing accurate measurement of the amplitude of the acoustic pressure response.

Chapter 3.

Acoustic Response of Patterned Metallized paper

3.1. Introduction

We tested five distinct patterns of metallized paper in the experimental setup shown in Figure 3. Membranes in Figure 6 (a), (b), and (c) each had a square geometry and were clamped along their perimeters using a rectangular clamp and spacer (Figure 6 (f)), while membranes in Figure 6 (c) and (d) were clamped using a circular clamp (Figure 6 (g)) and a triangular clamp (Figure 6 (h)), respectively. The five individual patterns were subject to frequency sweeps by sending 16 frequencies from 500 Hz to 8 kHz in increments of 500 Hz and amplitudes of ±2 kV. We limited the frequency to 8 kHz due to the doubling effect discussed in Chapter 2 and limitations in the bandwidth of the amplifier and sampling rate of the data acquisition system. Thus, we consequently characterized the frequency response of the membranes over a range of 1 kHz – 16 kHz.

3.2. Discussion

The frequency response plots (Figure 7) show the standard deviation of the output acoustic pressure for the five patterns with seven samples for each pattern. For the

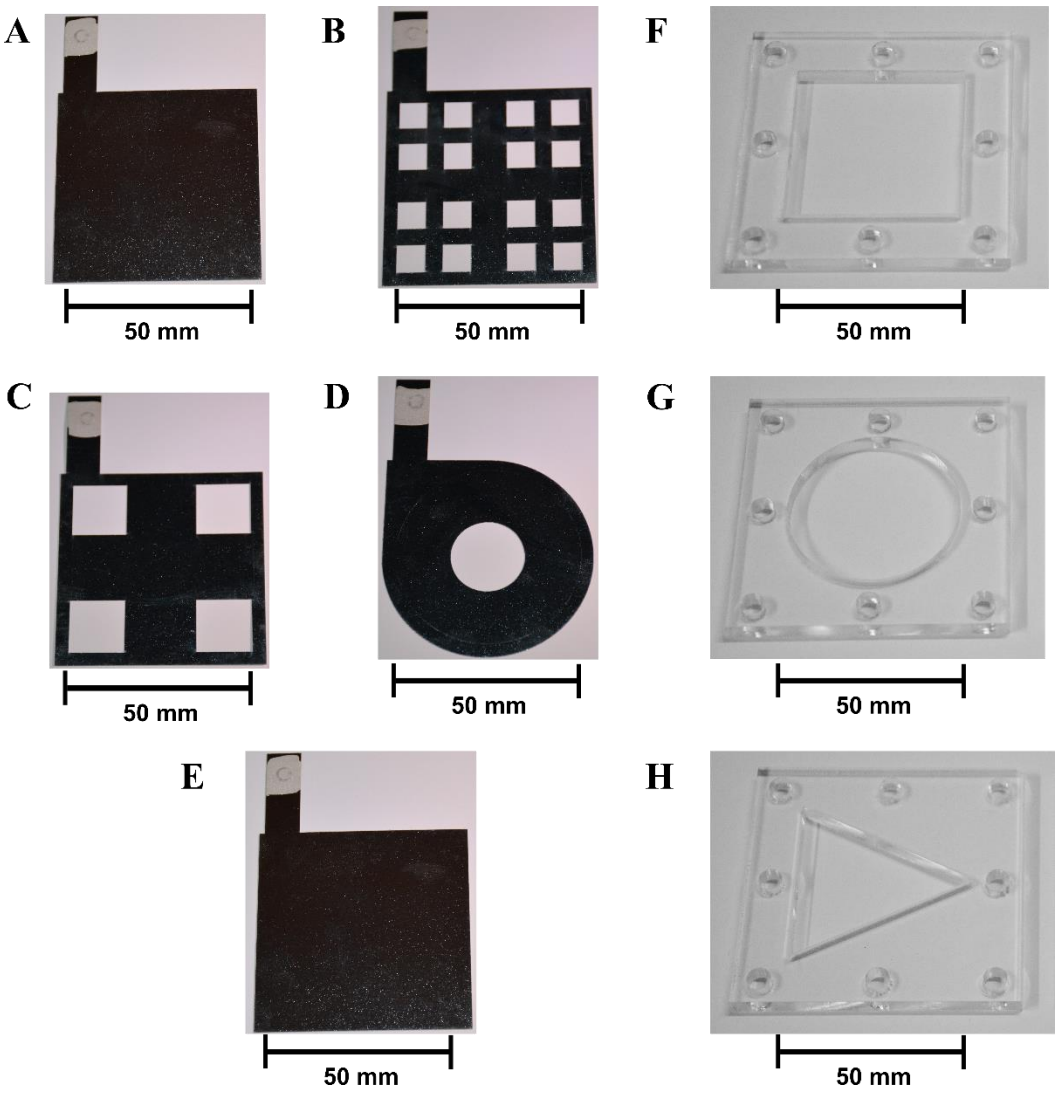

Figure 6: (a), (b), (c), (d) and (e) are images of patterned metallized paper used for experiments. Metallized paper was A-238 (thickness of 110 um) from AR Metallizing. (f), (g) and (h) show the acrylic fixtures used to clamp the metallized paper membranes along their edges. Clamp (f) was used for membrane (d); clamp (g) was used for membranes (a), (b), and (c); and clamp (h) was used for membrane (e).

membrane shown in Figure 6 (a), it is noticeable that the standard deviation was higher at 3 kHz and 4 kHz. This high standard deviation may be due to the fact that the pattern did not have any holes or cuts. Thus, when clamped in the setup (Figure 3 (b) and 3 (c)), the device had a nearly air-tight chamber that damped the response of the membrane due to viscous forces between the grounded electrode and the active membrane. By modifying patterns to have wider cuts (narrower widths of material), we see reductions in the simulated displacement at the low frequency (2 kHz) of forcing. Comparing the frequency response plots in Figure 7 (b) and 7 (c), we see that the pattern with larger width of the cross-like design (Figure 6 (c)) is louder at lower frequencies compared to the pattern in Figure 6 (b). The pattern in Figure 6 (d) is distinct with a circular clamp and the pattern in Figure 6 (e) has a triangular clamp but uses the same pattern shown in Figure 6 (a) with a different clamp. The difference in the frequency response of these patterns can only be credited to the different clamping conditions.

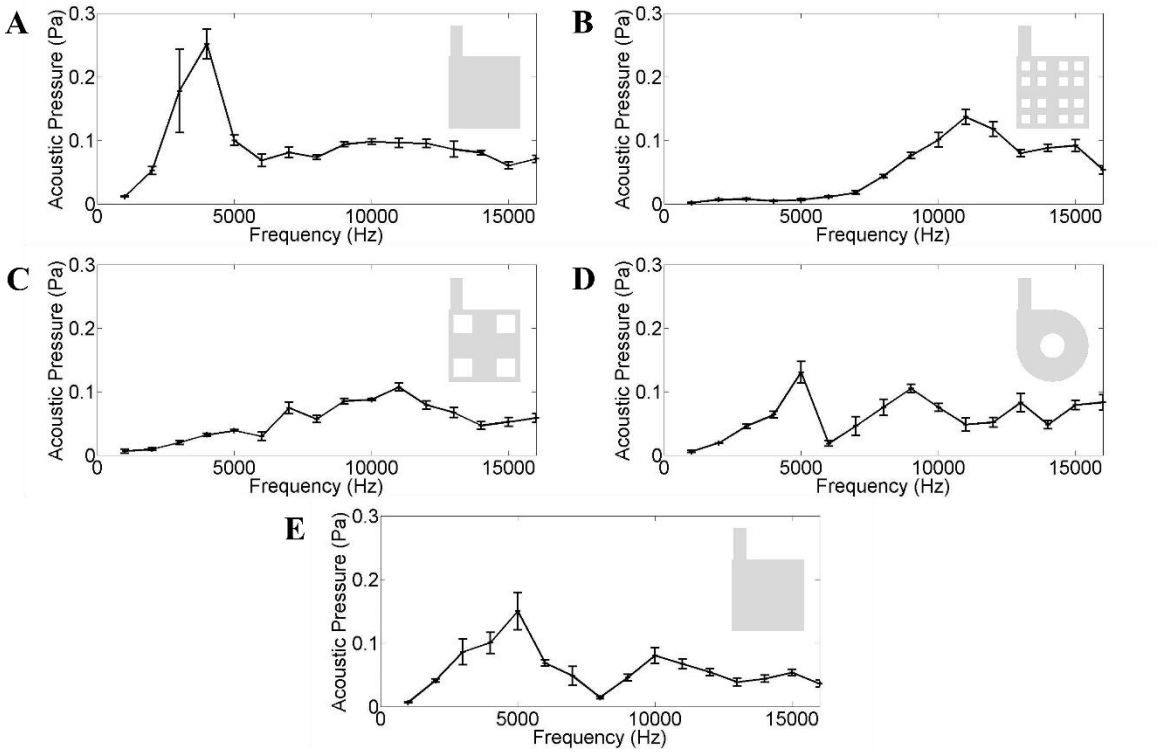

Figure 7: (a), (b), (c), (d) and (e) are frequency response plots for the respective geometric patterns shown in Figure 3 (a), (b), (c), (d) and (e)**.** The error bars are ± 1 standard deviation with seven distinct samples taken on the same device for each pattern.

Chapter 4.

Applications

The analysis of the membranes shown in Chapter 3 may be potentially useful in developing methods for detection and identification of objects. The ability to make patterns with different frequency responses points to the fact that encoding and changing the information on the membranes is possible by modifying their structure. This information is accessible when we subject the membranes to electrostatic excitation and measure the resulting acoustic response. The change in the response of the membranes to minute alterations in the pattern is significant, thus enabling these designs for use as anti-tampering devices. The configuration of electrodes has similarities with early designs of electrostatic speakers. These devices may also be useful as inexpensive speakers for smart packaging with their simple fabrication.

4.1. Loudspeaker

4.1.1. Experimental Setup

By playing audio notes through two different patterns with selective responses in separate frequency ranges, we demonstrate how patterned metallized paper can function as a speaker with tunable responses. For Patterns 1 and 2 chosen from Figure 3, we applied electrical signals corresponding to the tunes from two nursery rhymes: “Mary Had a Little Lamb” and “Twinkle Twinkle Little Star”. The electrical signals generated through MATLAB for these tunes are in two different octaves: one in the range of 1 kHz – 2.1 kHz and the second in the range of 4 kHz – 8.2 kHz. The responses for the first octave will be in the range of 2 kHz – 4.2 kHz and for the second octave it will be in the range of 8 kHz – 16 kHz. We made the patterns from 155-um thick metallized papers also provided by AR Metallizing. We chose a thick paper so that the resonance frequency of the plain paper lies in the octave with frequency range of 2093 Hz (C_7 Note) to 3951.07 Hz (B_7 Note). Compared to the response in Figure 7 (a) with 100-um thick paper in which the resonance occurred at 4 kHz, the thicker paper displays resonance at 3 kHz which is in our designation for octave 1.

We applied a voltage correction to the input signals similar to those shown in Figure 4 only at the input notes of the individual rhymes, and we used the setup shown in Figures 2 and 3 with the same experimental parameters. We also made a version of 12 Variations of “Twinkle Twinkle Little Star” ("Ah, Vous Dirai-je, Maman" KV 265) by Mozart. The objective with the last rhyme is to show the effectiveness of the membranes as acoustic filters when the input signals have two components, namely the bass and

treble clef notes. Due to the limitations on the sampling rate of the audio output, these complex waveforms when captured acoustically do not have enough data points to represent the actual waves with high acoustic fidelity. Instead, we play the notes in an alternating fashion (i.e., a bass note followed by a treble note, a bass note, etc.).

4.1.2. Results and Discussions

The pattern in Figure 6 (a) has more audible responses at lower frequencies, and the pattern in Figure 6 (b) has more audible responses at higher frequencies. The differences in responses at lower and higher frequencies are more distinguishable for the first pattern. Figure 8 shows the distinct filtering of both patterns and acoustically distinguishes them on the basis of how audible a particular rhyme sounds when played. This is noticeable in Figure 9, 10 and 11 in the acoustic responses of the membranes for the respective tunes.

With the technique for modifying the diaphragms presented in this work, there is potential to create electrostatic speakers with selective responses in desired or required spectrums of frequency. A good speaker has a flat response throughout the audible spectrum in order to have balanced audio output. With a plain diaphragm, getting a balanced response is achievable by modifying the material properties and dimensions along with extensive acoustic analysis. By using our patterning techniques, we can also change the shape and or boundary-clamping conditions to alter the audible characteristics of the diaphragm. There is potential to create a diaphragm, which is an assembly

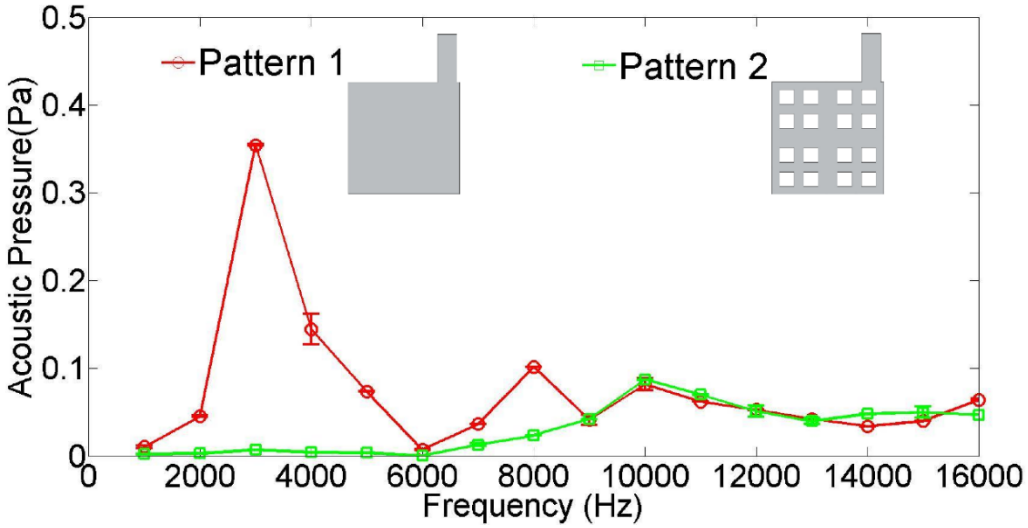

Figure 8. FFT showing frequency responses for patterns 1 and 2 in Figure 3 (a) and (b)**,** respectively using paper with a thickness of 155 um.

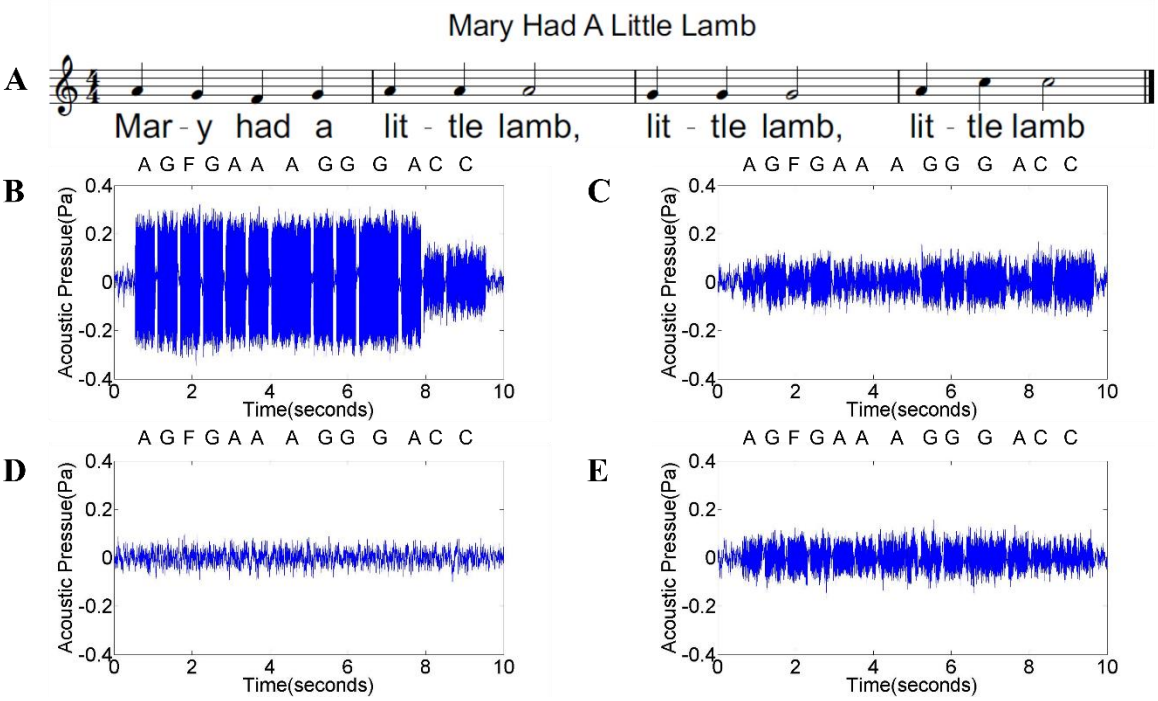

Figure 9: Audio outputs from devices playing "Mary Had a Little Lamb". (a) Musical staff for "Mary Had A Little Lamb" with notes that are octaves below those delivered to the devices. (b) Acoustic response of Pattern 1 to electrical signals in the frequency range of 1 kHz-2 kHz (i.e., A=1.76 kHz) with acoustic responses in the frequency range of 2 kHz-4 kHz. (c) Acoustic response of Pattern 1 to electrical signals in the frequency range of 4 kHz-8 kHz (i.e., A=3.52 kHz) with acoustic responses in the frequency range of 8 kHz-16 kHz. (d) Acoustic response of Pattern 2 to electrical signals in the frequency range of 1 kHz-2 kHz (i.e., A=1.76 kHz) with acoustic responses in the frequency range of 2 kHz-4 kHz. (e) Acoustic response of Pattern 2 to electrical signals in the frequency range of 4 kHz-8 kHz (i.e., A=3.52 kHz) with acoustic responses in the frequency range of 8 kHz-16 kHz.

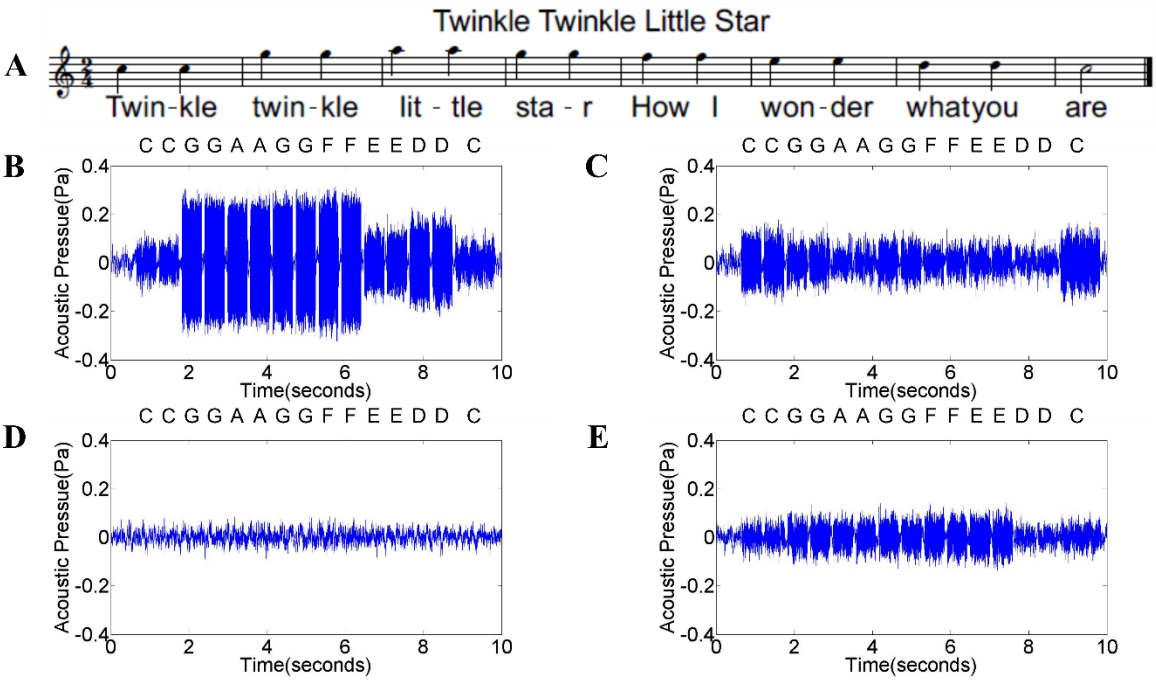

Figure 10: Audio outputs from devices playing "Twinkle Twinkle Little Star". **(**a) Musical staff for "Twinkle Twinkle Little Star" with notes that are octaves below those delivered to the devices. (b) Acoustic response of Pattern 1 to electrical signals in the frequency range of 1 kHz-2 kHz (i.e., A=1.76 kHz) with acoustic responses in the frequency range of 2 kHz-4 kHz. (c) Acoustic response of Pattern 1 to electrical signals in the frequency range of 4 kHz-8 kHz (i.e., A=3.52 kHz) with acoustic responses in the frequency range of 8 kHz-16 kHz. (d) Acoustic response of Pattern 2 to electrical signals in the frequency range of 1 kHz-2 kHz (i.e., A=1.76 kHz) with acoustic responses in the frequency range of 2 kHz-4 kHz. (e) Acoustic response of Pattern 2 to electrical signals in the frequency range of 4 kHz-8 kHz (i.e., A=3.52 kHz) with acoustic responses in the frequency range of 8 kHz-16 kHz.

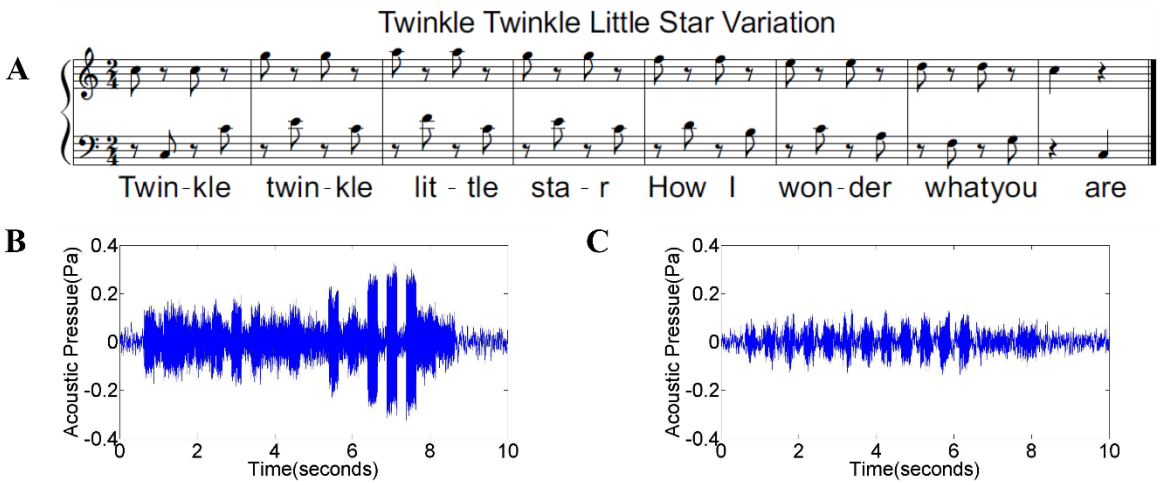

Figure 11: Audio output from Patterns 1 and 2, playing a variation of "Twinkle Twinkle Little Star" which has alternating notes in high and low frequencies. (a) Musical staff for "Twinkle Twinkle Little Star variation", which has notes in the treble clef and bass notes played alternately. (b) Measured acoustic response for Pattern 1 with the notes in the treble clef ranging from 4 kHz-8 kHz and bass notes ranging from 1 kHz- 1.76 kHz. (c) Measured acoustic response for Pattern 2 with the notes in the treble clef ranging from 4 kHz-8 kHz and bass notes ranging from 1 kHz- 1.76 kHz.

of smaller membranes with selective frequency responses in different spectrums such that the whole assembly of membranes would have a flat response over the entire frequency spectrum.

By using metallized paper as the membrane, there is potential to make inexpensive speakers which are environmental friendly by avoiding the use of plastic sheets [20]. The diaphragms in electrostatic speaker are conductive so that it is possible to place charges on it, which requires coating the plastic with a conductive material like graphite [12] in some cases. This step is not required in our design, as metallized paper is commercially available. This design has simpler construction issues compared to push-pull type electrostatic transducers [15]. Nonetheless, using this design transfers complexity to the amplifiers, which would need to halve the frequencies of the AC electrical signals.

4.2. Barcode Scanner

4.2.1. Introduction

Barcode technology is a method of automatic identification and data capture (AIDC), similar to that associated with radio-frequency identification, smart cards, or integrated circuit cards. These technologies help identify an object or an entity by analyzing images or radio waves. In addition to the conventional methods of AIDC, there are opportunities to build low-cost, paper-based systems for unique identification that have responses compatible with human-based modes of sensing. We envision patterned paper-based substrates for acoustic identification. This novel method of identification might be an alternative to barcode and RFID (radio frequency Identification).

A barcode encodes information in a visual pattern, which is readable by a machine or a scanner. Barcodes are useful for tracking products and control of inventory. A barcode scanner reads the data off the barcode by illuminating the code with light and detects the reflected signal [21]. The decoder receives and interprets the reflected signal, validates the barcode using a binary code, and converts the measurement to text. The scanner delivers this converted text to a computer, which has a software database with information for the maker, cost, and quantity of manufactured goods.

4.2.2. Experimental setup

To demonstrate a possible implementation of our novel technique, we patterned a 50-mm x 50-mm piece of metallized paper (Figure 12 (a)) to serve as the main active

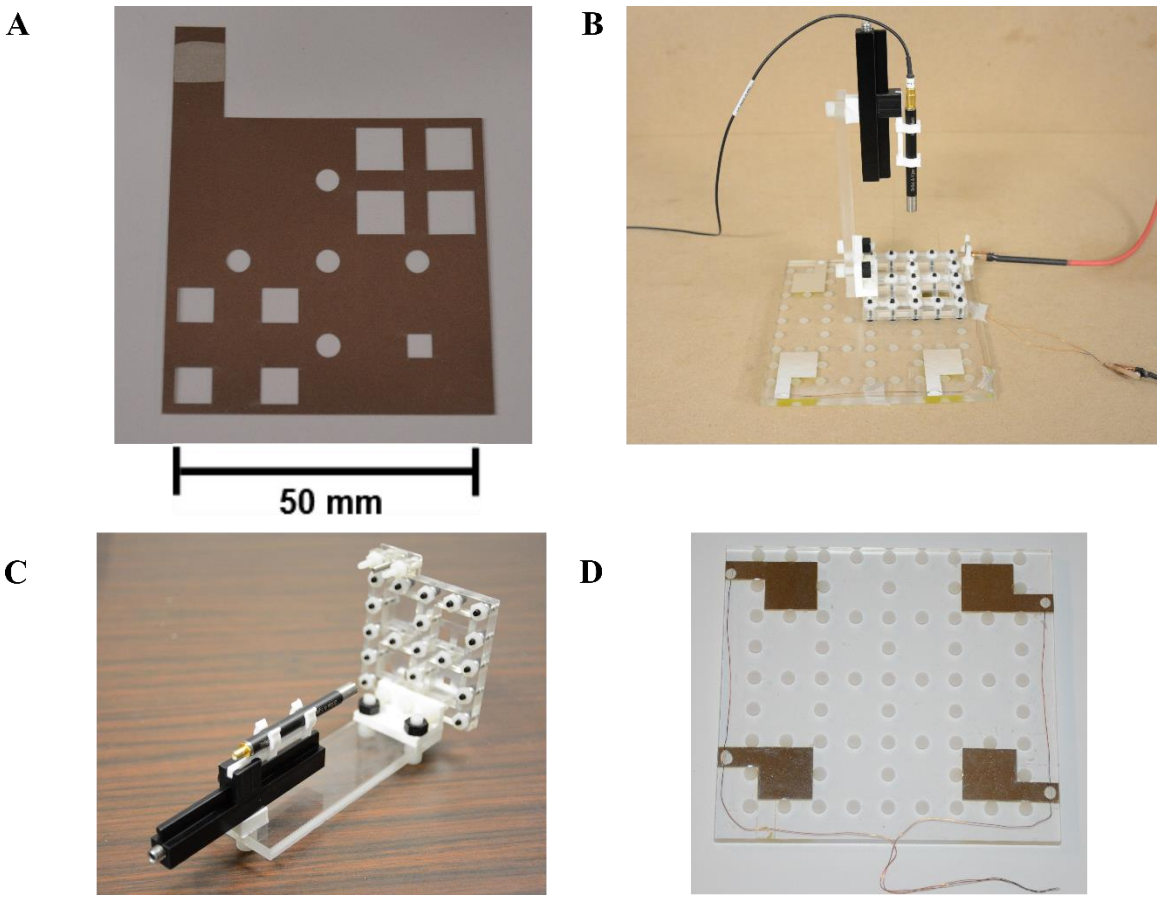

Figure 12: (a) Metallized paper from AR Metallizing A-238 (thickness of 110 um) with four 20-mm x 20-mm patterns cut using a laser cutter to the main component of the scanner. (a) Photo of experimental setup. (b) Scanner consisting of patterned metallized paper as an active electrode and a microphone perpendicular to plane of membrane. (c) Acrylic base with four Barcodes consisting of four grounded pieces of metallized paper (same as (a)) with electrical connections made using thin-grade copper wires and conductive adhesive.

component of a scanner. The scanner consisted of the patterned metallized paper, a clamp with two acrylic pieces held together with socket screws, and a microphone mounted perpendicular to the face of the metallized paper (Figure 12 (b)). This setup resembled a commercial hand-held scanner. The microphone was 55 mm away from the active electrode, the distance between the ground and active electrode was 4.4 mm, and the input voltage was ± 2 kV. Four grounded electrodes in placed in different corners of a rectangular region served as the barcodes. The four barcodes with four 20 mm x 20 mm grounded pieces of metallized paper were fixed to an acrylic sheet by double-sided tape (Figure 12 (c)). Figure 14 shows the schematic of the demonstration.

4.2.3. Results and discussions

Figure 15 shows the position of the scanner for detecting the four barcodes. Each grounded piece of metallized paper acted as a key component of the barcode. With the scanner placed on a barcode, only one of the four patterns on the scanner was directly opposite to a grounded region. For example, when the scanner was positioned across from barcode 1, only pattern 1 of the membrane was excited. Figure 15 (a) shows the Frequency response of the scanner membrane for the four possible positions or barcodes. The acoustic responses were distinct when measured at 5 kHz. In the demonstration video, we detected the barcodes at that frequency by sending input AC signals at 2.5 kHz (Figure 1 (a)).The upper and lower limits for the amplitude of acoustic pressure are set in the LabVIEW program for successful detection of the four barcodes (Figure 15 (b)).

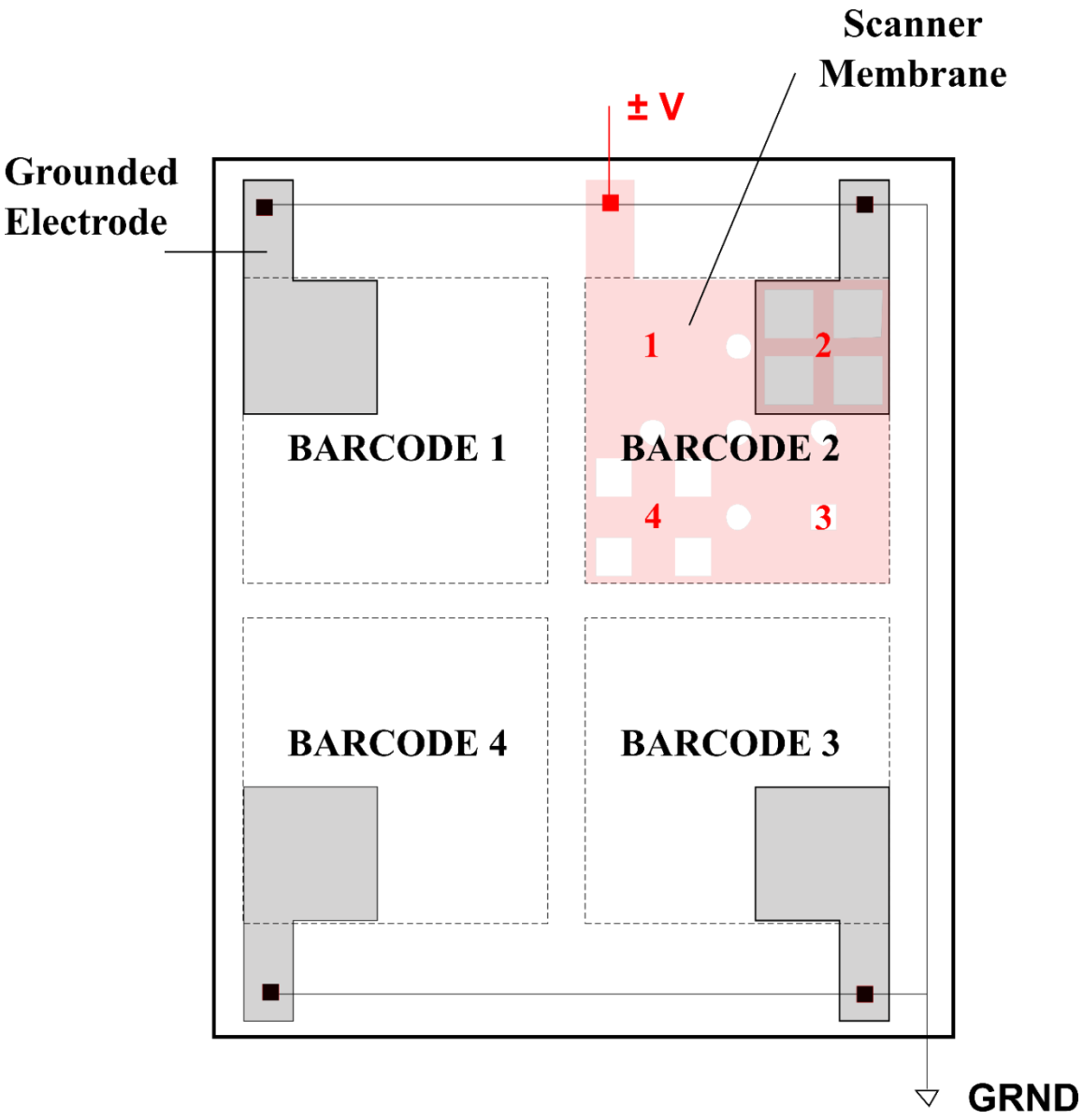

Figure 13: Schematic showing working of demonstration where each barcode excites only one of the patterns on the scanner membrane in Figure 13 (a).

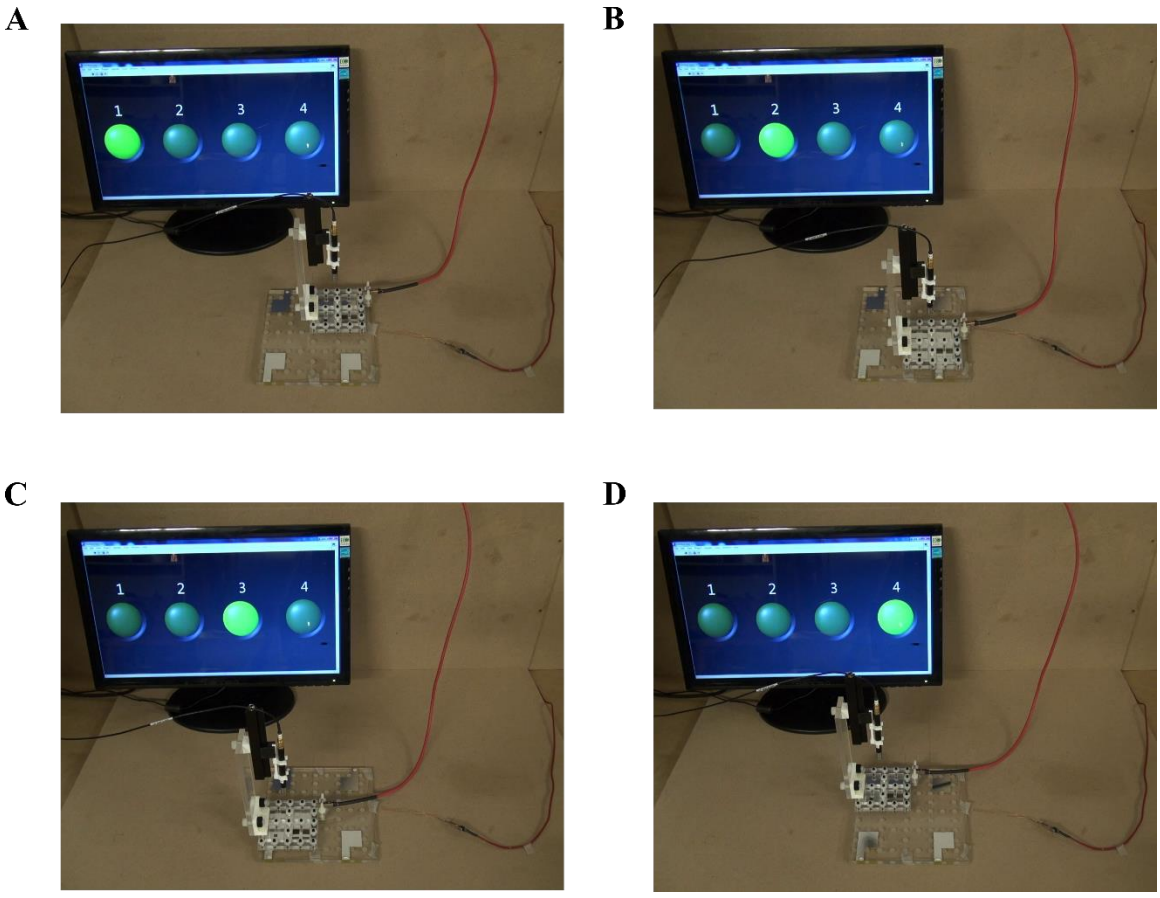

Figure 14: Snapshots of demonstration showing detection of barcodes and the position of scanner. (a), (b), (c), and (d) show detection of barcodes 1, 2, 3 and 4 respectively as shown on the screen by using a LabVIEW program.

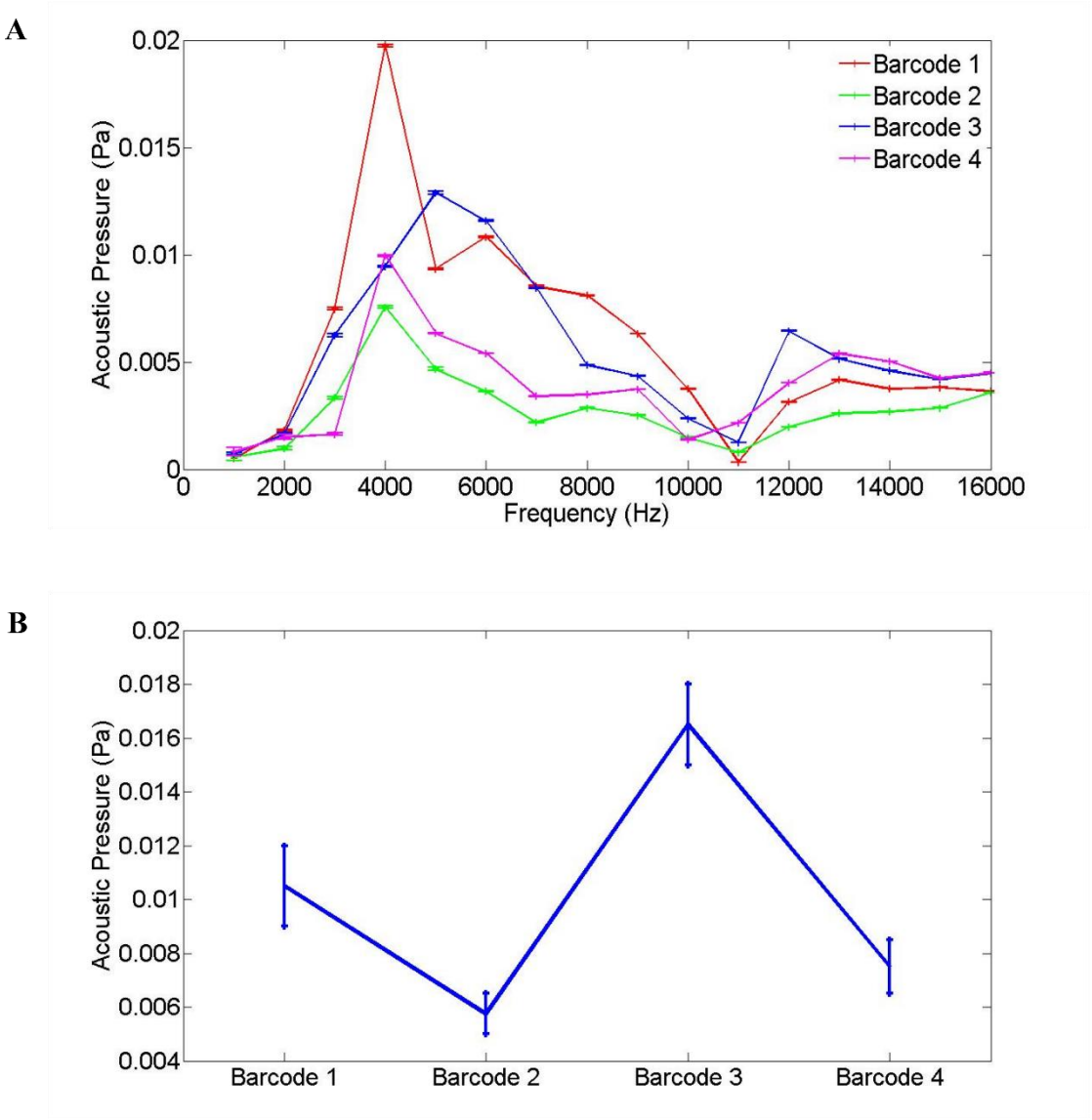

Figure 15: (a) Plot displaying responses of four barcode/patterns made from 110 um-thick metallized paper with the patterns easily distinguishable at 5 kHz. (b) The error bars show the upper and lower limits (thresholds) of acoustic pressure set in LabVIEW for detection of the four barcodes at 5 kHz.

There are different permutations and combinations possible depending on the arrangement of the grounded metallized pieces. One or more grounded metallized pieces may constitute one barcode that excites the respective number of patterns on the scanner membrane, which in our case is one pattern for one barcode. The present case has four patterns in the scanner membrane, which can possibly increase in number, depending on the number of objects or entities to detect. It should also be possible to compare the responses of the patterns at more than one frequency. Though this increases the complexity of the detection program, it also creates opportunities for detecting more complex barcode arrangements without increasing the number of patterns on the scanner membrane. It should also be possible to reduce the size and consumption of power of such scanning systems by moving the microphone closer to the membrane and by reducing the distance between the membrane and the grounded electrode.

Current laser scanners and CCD scanners operate by measuring the reflected light off a barcode and then converting it to a sequence of binary numbers that the computer recognizes. The decoding of reflected light to numbers requires a separate decoder circuitry to analyze the data [22]. In addition, these systems require line of sight, which may not be necessary for advanced acoustic detection. Overall, this idea and its application are in their infancy with potential to miniaturize the design, make them inaudible to humans (i.e., shift to ultrasonic frequencies), and improve resolution/accuracy.

4.3. Security and anti-tamper device

4.3.1. Motivation

As shown in Figure 7, we can create patterns with selective frequency response, which is analogous to encoding information on membranes. The frequency response information might be of potential importance for security devices. The membrane might be a key and when slid into a reader, it would vibrate in an identifiable way as described in Figure 3. Similar to the barcode application, we would be able to check the response of the key or membrane at certain frequencies and the door would unlock. The membrane would act as an information carrier, with shape-dependent memory. It might be useful to code information in terms of frequency response of the membrane to convey encrypted information to an intended recipient [23], which only the recipient might view or decode when used in similar fashion to that described in Figure 3 (b).

4.3.2. Experimental Setup

By performing thin incisions or cuts on a metallized paper membrane, we highlight the effectiveness of metallized paper as a security and anti-tamper device. The goal of this demonstration is to show that with small cuts, the response of the membrane changes significantly. We use the setup depicted in Figure 3 and pieces of 110-um thick metallized paper with slits of different lengths cut in them using a laser cutter. Patterns in Figure 16 (a), (b), and (c) have a 1-mm x 10-mm cut, a 1-mm x 30-mm cut, and a 1-mm x

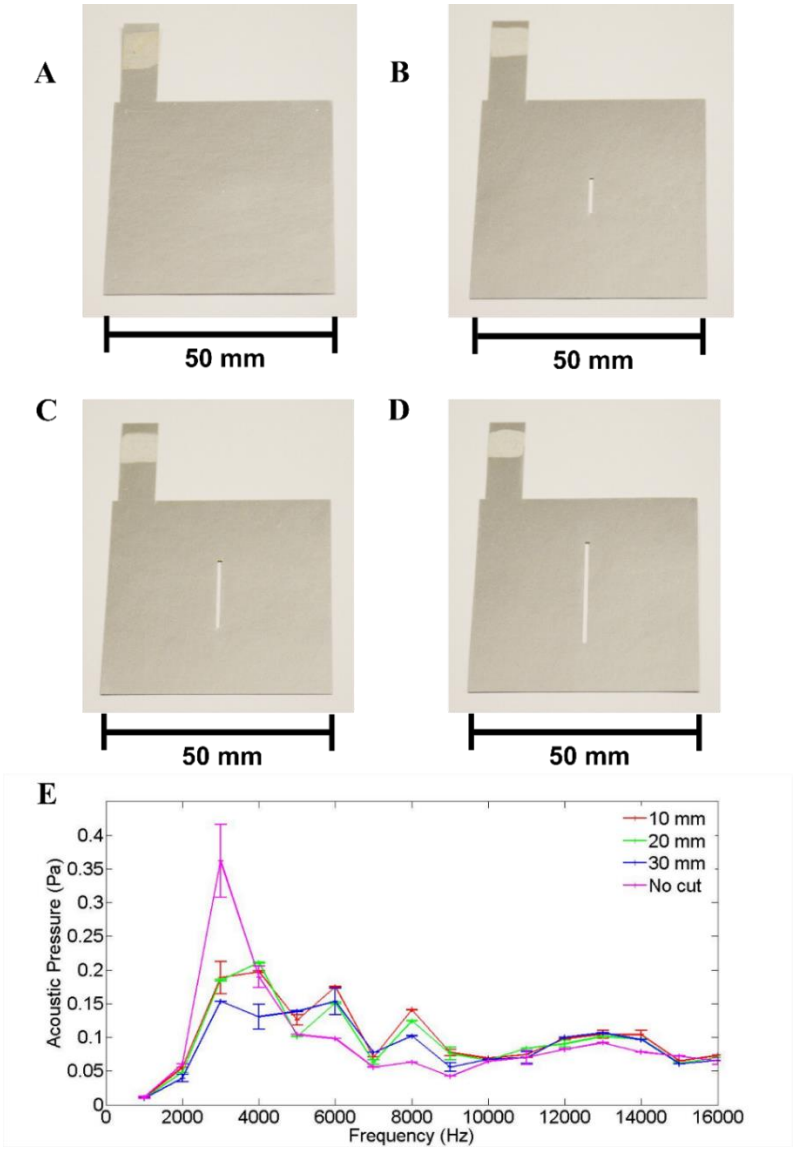

Figure 16: Images of 110-um thick metallized paper from AR Metallizing with slots/cuts, along with measured frequency responses. (a) Image of a sheet of metallized paper without a cut. (b) Image of a sheet with a 1-mm x 10-mm slot. (c) Image of a sheet with a 1-mm x 20-mm slot. (d) Image of a sheet with a 1-mm x 30-mm slot (e) Plot comparing frequency responses of patterns in (a), (b), (c) and (d).

20-mm cut, respectively. Figure 17 shows the experimental setup for the demonstration video displaying the effect of a small incision made using a scalpel on the response of the membrane. We sent an input AC signal of ± 2 kV at 2 kHz to the membrane and measured the response at 4 kHz.

4.3.3. Results and Discussions

The plot in Figure 16 (e) shows the relative change in the frequency response, and the change was most evident close to the resonant frequency of the uncut membrane. The resonance occurred at 3 kHz (slightly less than that shown in Figure 7 (a)). We hypothesize this change in resonance may have resulted from aging (experiments were 3 months apart) or humidity [24]. At 3 kHz, there is a 50 % reduction in the response of the membrane with a 10-mm cut, although we only removed 4% of the original area. Figure 18 demonstrates how the membrane had a response of 0.0865 Pascals (Figure 18 (a)) without a cut and a response of 0.0990 Pascals (Figure 18 (c)) with a small incision of 16 mm made by a scalpel. When monitoring the acoustic pressure at 4 kHz, we saw a 12% increase in the acoustic response. We believe the enhanced amplitude was due to the increased freedom of the membrane to move back and forth without the airtight chamber of entrapped air.

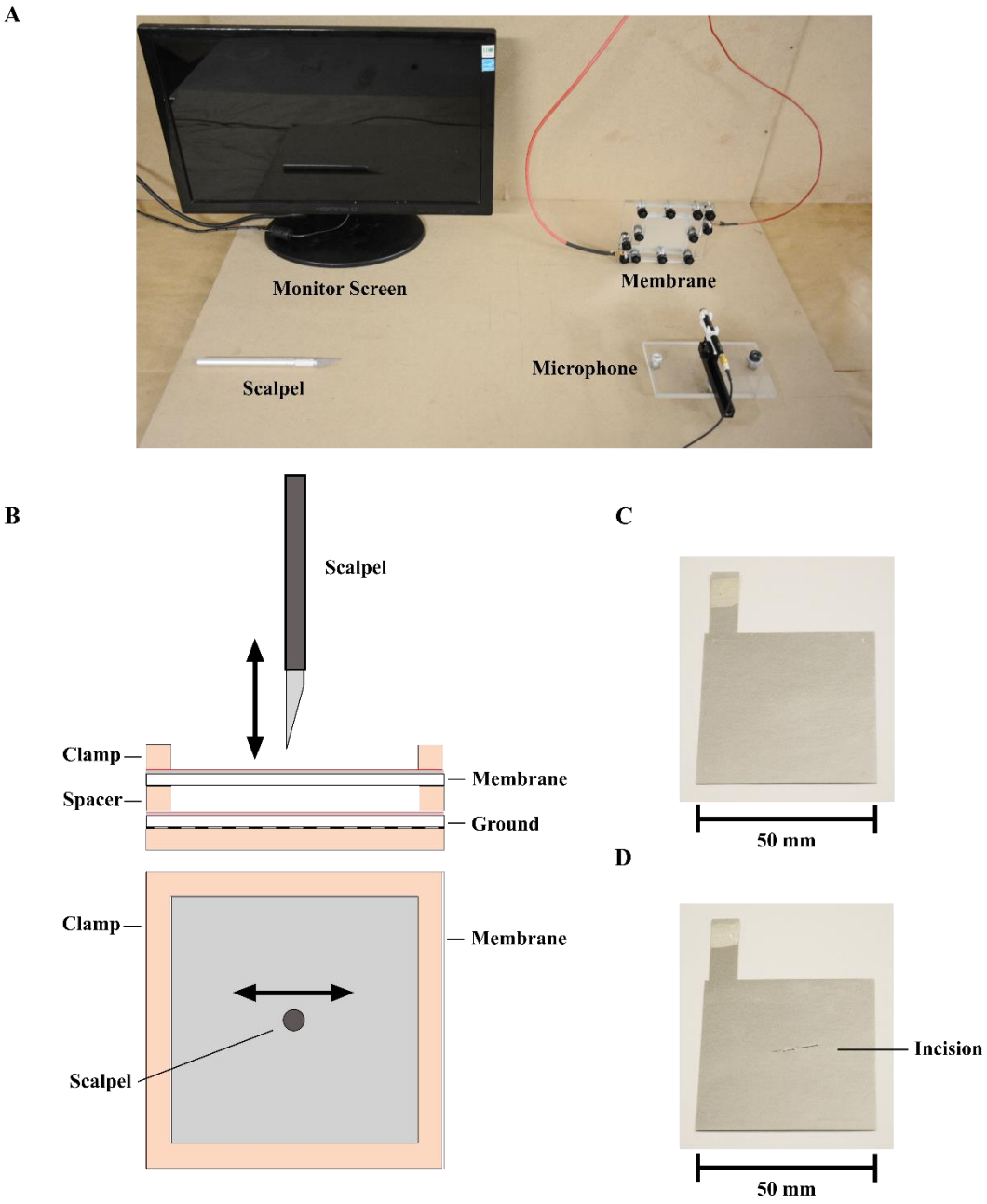

Figure 17: Setup description for demonstration/anti-tamper video using metallized paper with a thickness of 110 um. (a) Image of experimental setup with scalpel, electrode setup and microphone. (b) Schematic describing the process of incision made using a scalpel on metallized paper. (c) Image of paper without a cut. (d) Image of paper with cut.

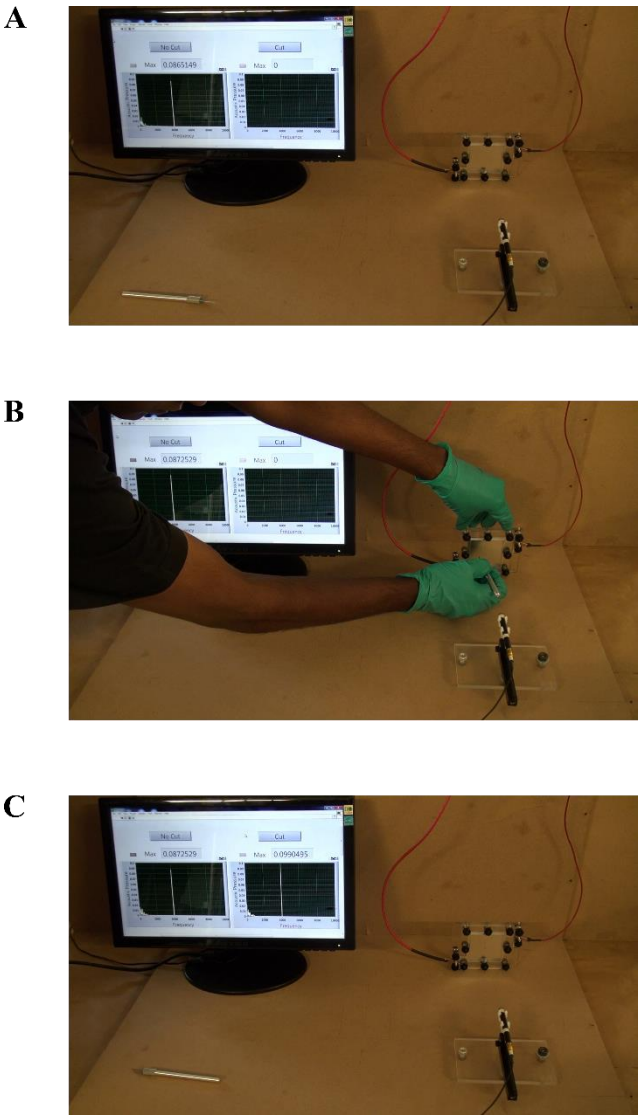

Figure 18: Snapshots of the demonstration for an input voltage of ± 2 kV at 4 kHz. (a) Image showing the amplitude of acoustic pressure at 0.0865 Pascals with no incision. (b) Image showing process of cutting the paper with a scalpel. (c) Image showing the amplitude of acoustic pressure at 0.0990 Pascals with incision.

Chapter 5.

Conclusions and Future Work

5.1. Conclusions

The present work successfully displays the ability to produce sound from a membrane of metallized paper with an oscillating source of high voltage. We were able to transform or modify the vibrational characteristics of the membrane by cutting it in different shapes and varying clamping conditions. We tested five such patterns and presented their distinct frequency responses. The initial demonstrations showed potential applications of this technology in electrostatic speakers, anti-tampering devices, and acoustic barcodes. With further study and research, it should be possible to create membranes with patterns that would have predictable frequency responses.

5.2. Future Work

Future work would include characterizing the frequency response of patterned metallized papers with different geometric parameters (gap, length, width, and thickness) and material parameters (Young's modulus and Poisson's ratio). Simulations accounting for damping and tension in the membrane would also improve the predictive accuracy. By comparing conventional diaphragm membranes of metallized PET/Mylar found in

common electrostatic speakers to metallized paper, we might also better gauge the the potential of metallized paper as an acoustic membrane. Finally, development of an inexpensive circuit to produce high voltage at the required frequencies would make barcode scanning and security devices, less expensive and more compact for commercial application.

References

[1] A. W. Martinez, S. T. Phillips, G. M. Whitesides, and E. Carrilho, "Diagnostics for the Developing World: Microfluidic Paper-Based Analytical Devices," *Anal. Chem.*, vol. 82, no. 1, pp. 3–10, Jan. 2010.

[2] E. J. Maxwell, A. D. Mazzeo, and G. M. Whitesides, "Paper-based electroanalytical devices for accessible diagnostic testing," *MRS Bull.*, vol. 38, no. 04, pp. 309–314, 2013.

[3] F. Eder, H. Klauk, M. Halik, U. Zschieschang, G. Schmid, and C. Dehm, "Organic electronics on paper," *Appl. Phys. Lett.*, vol. 84, no. 14, pp. 2673–2675, Apr. 2004.

[4] R. Martins, A. Nathan, R. Barros, L. Pereira, P. Barquinha, N. Correia, R. Costa, A. Ahnood, I. Ferreira, and E. Fortunato, "Complementary Metal Oxide Semiconductor Technology With and On Paper," *Adv. Mater.*, vol. 23, no. 39, pp. 4491–4496, Oct. 2011.

[5] S. Yun, S.-D. Jang, G.-Y. Yun, J.-H. Kim, and J. Kim, "Paper transistor made with covalently bonded multiwalled carbon nanotube and cellulose," *Appl. Phys. Lett.*, vol. 95, no. 10, p. 104102, Sep. 2009.

[6] R. Martins, P. Barquinha, L. Pereira, N. Correia, G. Gonçalves, I. Ferreira, and E. Fortunato, "Write-erase and read paper memory transistor," *Appl. Phys. Lett.*, vol. 93, no. 20, p. 203501, Nov. 2008.

[7] A. D. Mazzeo, W. B. Kalb, L. Chan, M. G. Killian, J.-F. Bloch, B. A. Mazzeo, and G. M. Whitesides, "Paper-Based, Capacitive Touch Pads," *Adv. Mater.*, vol. 24, no. 21, pp. 2850–2856, Jun. 2012.

[8] Z.-S. Wu, A. Winter, L. Chen, Y. Sun, A. Turchanin, X. Feng, and K. Müllen, "Three-Dimensional Nitrogen and Boron Co-doped Graphene for High-Performance All-Solid-State Supercapacitors," *Adv. Mater.*, vol. 24, no. 37, pp. 5130–5135, Sep. 2012.

[9] A. C. Siegel, S. T. Phillips, B. J. Wiley, and G. M. Whitesides, "Thin, lightweight, foldable thermochromic displays on paper," *Lab. Chip*, vol. 9, no. 19, p. 2775, 2009.

[10] P. Andersson, D. Nilsson, P.-O. Svensson, M. Chen, A. Malmström, T. Remonen, T. Kugler, and M. Berggren, "Active Matrix Displays Based on All-Organic Electrochemical Smart Pixels Printed on Paper," *Adv. Mater.*, vol. 14, no. 20, pp. 1460–1464, Oct. 2002.

[11] M. C. Barr, J. A. Rowehl, R. R. Lunt, J. Xu, A. Wang, C. M. Boyce, S. G. Im, V. Bulović, and K. K. Gleason, "Direct Monolithic Integration of Organic Photovoltaic Circuits on Unmodified Paper," *Adv. Mater.*, vol. 23, no. 31, pp. 3500–3505, Aug. 2011.

[12] H. Tian, T.-L. Ren, D. Xie, Y.-F. Wang, C.-J. Zhou, T.-T. Feng, D. Fu, Y. Yang, P.-G. Peng, L.-G. Wang, and L.-T. Liu, "Graphene-on-Paper Sound Source Devices," *ACS Nano*, vol. 5, no. 6, pp. 4878–4885, Jun. 2011.

[13] "History and Types of Speakers." [Online]. Available: http://www.edisontechcenter.org/speakers.html. [Accessed: 23-Sep-2015].

[14] J. Merhaut, *Theory of electroacoustics*. McGraw-Hill College, 1981.

[15] F. V. Hunt, *Electroacoustics: the analysis of transduction, and its historical background*. Acoustical Society of America, 1954.

[16] J. A. A, “Electrostatic loud-speaker,” US2631196 A, 10-Mar-1953.
[17] W. Szewczyk, K. Marynowski, and W. Tarnawski, “An Analysis of Young’s Modulus Distribution in the Paper Plane,” *Fibres Text. East. Eur.*, vol. Nr 4 (58), 2006.
[18] O. E. Öhrn, “Thickness variations of paper on stretching,” *Sven. Papperstidning*, vol. 68, no. 5, pp. 141–149, 1965.
[19] B. ISO, “536: 1997 Paper and board,” *Determ. Grammage*.
[20] “ESL 101: Electrostatic Theory and MartinLogan Speakers.” [Online]. Available: http://www.martinlogan.com/learn/electrostatic-speakers.php. [Accessed: 25-Sep-2015].
[21] M. S. Wang, “Line focus barcode scanner,” US5914477 A, 22-Jun-1999.
[22] R. A. Martino, “Digitizer for barcode scanner,” US5272323 A, 21-Dec-1993.
[23] M. A. Palacios, E. Benito-Peña, M. Manesse, A. D. Mazzeo, C. N. LaFratta, G. M. Whitesides, and D. R. Walt, “InfoBiology by printed arrays of microorganism colonies for timed and on-demand release of messages,” *Proc. Natl. Acad. Sci.*, vol. 108, no. 40, pp. 16510–16514, 2011.
[24] H. W. H. Jr, “The Moisture and Rate-Dependent Mechanical Properties of Paper: A Review,” *Mech. Time-Depend. Mater.*, vol. 4, no. 3, pp. 169–210, Sep. 2000.